Journal of Bio- and Tribo-Corrosion (2018) 4:59
https://doi.org/10.1007/s40735-018-0177-5

MCM-41 Supported Copper-Based Catalysts: Physicochemical Characterizations and Catalytic Performances in the Gas Phase Hydrogenation of Benzaldehyde

Mohammed Sadou[1,2] · Adel Saadi[1] · Khaldoun Bachari[3] · Rami Suleiman[4] · M. Hadj Meliani[2]

Received: 26 May 2018 / Revised: 21 July 2018 / Accepted: 16 August 2018 / Published online: 23 August 2018

Abstract
We are reporting in this study the preparation of copper-based catalysts supported on MCM-41 mesoporous molecular sieves with different Si/Cu ratios (10 and 50) via two steps: firstly, the synthesis of the mesoporous material MCM-41 by the hydrothermal method and secondly, the preparation of the supported catalysts by a wet impregnation method. The structural and textural properties of the supported catalysts were determined using the atomic absorption spectroscopy (AAS), Fourier transform infrared spectroscopy (FTIR), X-ray diffraction (XRD), N_2-physical adsorption, and scanning electron microscopy (SEM) techniques. The catalytic properties of the supported materials have been evaluated on the reduction reaction of benzaldehyde at atmospheric pressure and in the gas phase. The yields of the obtained hydrogenation and hydrogenolysis products (benzyl alcohol, toluene, and benzene) were highly dependent on the copper content and reaction temperature, and preferentially formed in the whole range of reaction temperatures 160–250 °C. The observed selectivity of the hydrogenation and hydrogenolysis reactions towards the production of various products suggests the existence of catalytic active species of different particle sizes in the two catalyzed reactions.

Keywords MCM-41 · Mesoporous material · Hydrogenation · Benzaldehyde · Copper

1 Introduction

The use of metals as catalysts represents nearly around 70% of all the catalytic processes because it intervenes in the chemical synthesis of valuable products such as basic chemicals, petrochemistry, and fine chemistry [1], in the energy production (hydrogen production and conversion, conversion of the biomass) [2], and in the processes of environmental protection (treatments of pollution of air and water) [3]. Supported and unsupported pure or mixed transition metal-containing catalysts (Ni, Pd, Pt, Cu, etc.) were the subject of many reported studies in literature on their preparation, characterization, mechanisms of action, and applications in all the quoted fields [4–6].

Researchers from the Mobil firm have introduced in 1992 a new family of mesoporous silica and alumina-silica compounds named by M41S class [7–10]. These materials have been resulted from the interaction of inorganic species (silicates, aluminosilicates) with a micelle structure produced by a cation surface-active agent (alkyl bromide or chloride trimethylammonium). Among these materials, MCM-41 possesses a hexagonal arrangement of uniformly sized mesopores. The MCM-41 materials are characterized by a high specific surface (about 1000 $m^2\ g^{-1}$), ordered silicate channels, high porosity with sizes of pores uniform and centered between 2 and 10 nm and walls of amorphous nature [7, 8]. It should, however, be noted that these materials have a low hydrothermal stability which limits their applications compared to zeolites, especially in catalysis owing to the lack of active sites. Therefore, great efforts have been focused on the surface modification of these materials aiming to expand the area of applications [11]. The

✉ M. Hadj Meliani
m.hadjmeliani@univ-chlef.dz

1 Laboratory of Natural Gas Chemistry, Faculty of Chemistry, University of Sciences and Technology Houari-Boumediene, P.O.Box 32, El-Alia, Bab-Ezzouar, Algiers, Algeria

2 LPTPM, Hassiba Benbouali University of Chlef, B.O.Box 151, 02000 Chlef, Algeria

3 Research Center in Analytical Chemistry and Physics (CRAPC), Bou-Ismail, PoBox 248, Tipaza, Algeria

4 Center of Research Excellence in Corrosion (CoRE-C), King Fahd University of Petroleum & Minerals (KFUPM), Dhahran 31261, Saudi Arabia

introduction of heteroatom in the hexagonal structure of the MCM-41 is one of the most effective ways to make the solids more active and selective in various reactions. Up to now, lots of elements have been used to dope the wall of MCM-41 such as Al, Fe, Zn, Ti, V, Cu, Ni, W, and Mn [12–14]. Especially, copper is among one of the most efficient transition metals in the catalytic hydrogenation reactions of various organic functional groups [15]. In particular, the catalytic selective hydrogenation of carbonyl compounds is an important reaction that leads to the synthesis of valuable intermediates and finished chemicals, such as the alcohol precursors used in the pharmaceutical industry, fine chemicals, cosmetic. [16, 17].

The benzaldehyde hydrogenation to benzyl alcohol is one of the most important industrial reactions due to the remarkable properties of aromatic alcohol such as strong polarity and low toxicity/volatility. It is generally used as solvent for paints and coating, pharmaceuticals [18], perfumes, flavors, and in the synthesis of a large number of fine chemicals [19, 20]. Recently, the several studies carried out on various catalysts for hydrogenation of benzaldehyde has been discussed in detail in Ref. [21]. Hydrogenation reactions in the vapor phase have higher conversions and facilitate the separation of products compared to liquid phase reactions, making them more industrially favorable.

The association of hydrogen to a suitable catalyst is a clean economic approach which allows the reduction of the carbonyl compounds. This catalytic hydrogenation of unsaturated substrates is one of the fundamental transformations into chemistry, employed in a multitude of industrial chemical processes [22, 23]. The development of robust catalysts with an excellent selectivity towards the carbonyl group is still a very challenging area of research, especially in the weak load applications of catalysts. Many unsaturated carbonyls are vulnerable to hydrogenation and instead the isomerization of C=C bond occurs under the conditions of the hydrogenation of C=O bond [24].

Since the catalytic properties of transition metal functionalized with MCM-41 depend on the structure, location, and nature of the embedded metal, the synthesized catalysts are usually characterized prior to the evaluation of their catalytic activity. In this paper, we report the hydrogenation of benzaldehyde catalyzed by MCM-41 impregnated by copper under mild experimental conditions. The effects of various reaction parameters such as time, temperature, nickel loading during conversion, and product selectivity were also carefully studied and discussed.

2 Experimental

2.1 Synthesis

2.1.1 Materials

The following chemicals were used for the preparation of copper-containing MCM-41 catalysts with different Si/Cu molar ratios: tetraethyl orthosilicate (TEOS-98%, Aldrich), cetyltrimethylammonium bromide (CTAB-99%, Aldrich), and copper nitrate ($Cu(NO_3)_2{\cdot}3H_2O$, M.W: 241.6, Aldrich).

2.1.2 Synthesis of Pure-Silica MCM-41

Pure-silica MCM-41 material was synthesized hydrothermally as reported by Parida et al. [25] with typical (molar) gel compositions and using a quaternary ammonium cation C_{16}TMABr dissolved in water at room temperature [26]. The molar ratios of the components are as follows: CTMAB: 0.12, NH_4OH: 9.3, TEOS: 1, H_2O: 130.

The mixture was stirred at 60–80 °C for 24 h and the obtained precursor was filtered and washed with hot water. The surfactant organics were then extracted by washing and filtering using ethanol and water successively for 2 h at 80 °C. The drying of the solid obtained was achieved at 100 °C for 24 h and the final mesoporous material MCM-41 was obtained by calcination at 550 °C for 6 h.

2.1.3 Synthesis of Cu/MCM-41 Catalysts

The mesoporous Cu/MCM-41 molecular sieves with Si/Cu molar ratios of 10 and 50 were synthesized by an impregnation method, which is a simple method adopted for preparing the solids containing transition metals located at extra framework of the mesoporous MCM-41 molecular sieves. This method involves the deposition of metal oxides on a support via an impregnation step and starting from the aqueous solutions (nitrates, chlorides) [27]. In our case, the calcined MCM-41 samples used as a support were impregnated by an aqueous solution of $Cu(NO_3)_2$, $3H_2O$. The precursors were stirred, washed with water, evaporated, dried then overnight at 100 °C, and finally calcined in air flow at 550 °C for 6 h. The prepared samples are called *n*-Cu/MCM-41 (where $n = 10, 50$).

2.2 Catalysts Characterization

The determination of copper content was carried out by the atomic absorption spectrometry (AAS) technique using a Perkin-Elmer 2380 spectrophotometer. The settlement

of solids in the analyte was carried out using a mixture of nitric and hydrochloric acid until total dissolution.

The surface areas of the catalysts were estimated using the Brunauer–Emmett–Teller (BET) method and the pore size/volume were calculated by the Barrett–Joyner–Halenda (BJH) method using a multipoint N_2 adsorption–desorption method at − 196 °C on an Autosorb (Micromeritics-ASAP2020). The identification of crystalline compounds and the determination of average crystallite size were carried out by an X-ray diffraction (XRD) using Rigaku Miniflex diffractometer with Cu-K_α monochromatic radiation. X-ray diffraction XRD patterns of powdered samples were taken in the 2θ range 1°–80° at a rate of 2°/min in steps of 0.02°. The average size of the copper particles was calculated using the Scherrer equation with Warren's correction for instrumental line broadening [28]. The fourier transform infrared spectra of all samples were recorded on a Phillips 9800-FTIR spectrometer with a KBr pellet technique. The scanning electron microscopy (SEM) surface images of the prepared samples were observed using a JEOL-2000 electron microscope.

2.3 Catalytic Testing

The catalytic performances of the newly prepared materials were carried out in a fixed-bed glass tubular reactor at atmospheric pressure with 25 mg sample size and a total flow rate of 50 $cm^3\ min^{-1}$. The reactant gas feed consisted of 4.8 torr of benzaldehyde (Aldrich, 99.98%) and 250 torr of H_2. Benzaldehyde gas was obtained by bubbling H_2 in a liquid benzaldehyde maintained at a constant temperature (50 °C) in a suitable saturator. Before testing, the catalysts were in situ reduced for 4 h at 350 °C in flowing H_2 (flow rate of 20 $cm^3\ min^{-1}$).

The gaseous reactants and products were heated upstream and out-stream and analyzed on line by a FID gas chromatograph (Delsi IGC 121 ML) equipped with a 10% CP-SIL8 CB/Chromosorb W column. Each reaction temperature was maintained constant until the corresponding steady state was reached as indicated by the gas chromatograph analysis of the exit gases samples. For each catalyst, the reaction temperature was changed in a crossing order 160 °C, 250 °C, and 200 °C.

3 Results and Discussion

3.1 Physicochemical Characterizations

The results of the ultimate analysis by atomic absorption show that the molar concentrations of the metal ions Cu^{2+} present in the prepared catalysts were in concordance with those calculated theoretically, which explains why the near total of metal is impregnated on the support (Table 1). The specific surface areas (S_{BET}) were measured with BET method, and the pore volumes (V_p) and pore sizes (D_p) were calculated from the desorption branch with BJH method. The results depicted in Table 1 revealed that the specific surface area of pure-silica MCM-41 is 878 $m^2\ g^{-1}$ and the impregnation of copper species into the MCM-41 structure led to a decrease in the specific surface area. This value drastically decreased from 878 to 368 $m^2\ g^{-1}$ when the copper content increased from Si/Cu = 50 to 10 implying a decrease in the pores diameter from 2.8 to 2.5 nm and an increase in the pores volume from 1.29 to 1.54 $cm^3\ g^{-1}$, which explains why the metal particles distributed very well on the surface of the porous support MCM-41 and not inside these pores.

The distribution of pores size for both of the calcined catalysts is shown in Fig. 1. The distribution curves show a narrow and sharp peak with a pore size about 2–3 nm for 50-Cu/MCM-41 sample indicating the presence of a homogeneous and uniform pore size distribution. For 10-Cu/MCM-41 catalyst, the distribution curve shows a large and non-symmetric peak with a pore size of about 1–5 nm. The spread out distribution of the pores is significant in the formation of an inhomogeneous pore size.

Table 1 Surface properties of copper-loaded MCM-41

Catalysts	Si/Cu[a] (AAS)	S_{BET}[b] ($m^2\ g^{-1}$)	Dp[b] (BJH) (nm)	Vp[b] ($cm^3\ g^{-1}$)	d-spacing[c] (nm)	D[e] (nm)	Unit cell parameter[c], a_0 (nm)	Wall thickness[d] (nm)
MCM-41	/	878	2.8	1.54	2.45	–	2.83	0.03
50-Cu/MCM-41	46.8	593	2.7	1.47	2.44	2.7	2.82	0.12
10-Cu/MCM-41	10.4	368	2.5	1.29	2.44	4.7	2.82	0.32

[a]Atomic ratio obtained from chemical analysis

[b]Values obtained from nitrogen adsorption/desorption results

[c]Values obtained from XRD studies

[d]Wall thickness (t) = unit cell parameter (a_0) − pore size (Dp) [11]

[e]Average copper crystallites diameter calculated by Debye–Scherrer equations

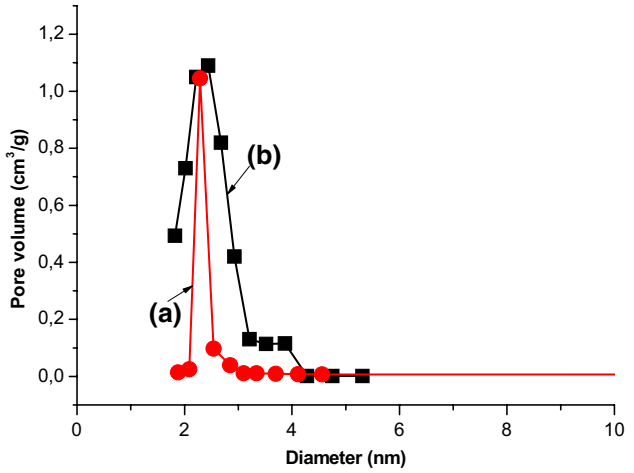

Fig. 1 Pore size distribution curves obtained by BJH method of calcined (*a*) 50-Cu/MCM-41 and (*b*) 10-Cu/MCM-41 catalysts prepared by impregnation method

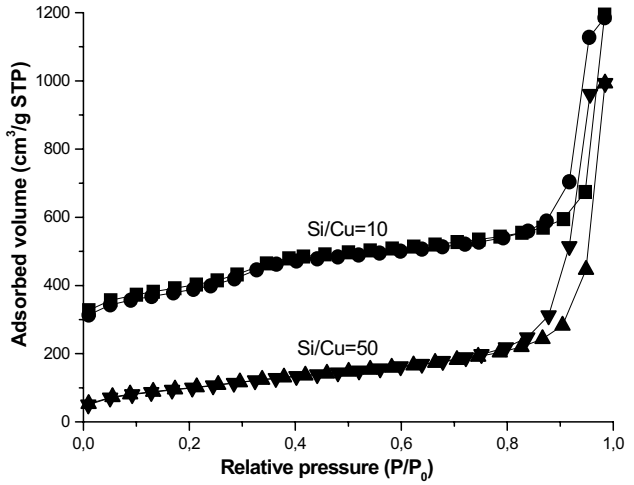

Fig. 2 Nitrogen adsorption–desorption isotherms of calcined *n*-Cu/MCM-41 catalysts (*n* = Si/Cu = 10 and 50)

Figure 2 represents the typical nitrogen adsorption–desorption isotherms of then-Cu/MCM-41 mesoporous catalysts. The results reveal that the isotherms obtained are of type IV as per the IUPAC classification [29], in which the hysteresis loop is of the H1 type, and are characteristic of mesoporous materials with uniform mesopores. The adsorption and desorption isotherms obtained on 10-Cu/MCM-41 show a sharp inflection in the relative pressure (P/P_0) ranging from 0.3 to 0.4, which is due to the capillary condensation of nitrogen within the mesopores [30]. After filling the mesopores, it can be seen that the adsorption and desorption isotherms are not flat, indicating that the external surface area of MCM-41 catalysts is not small. In agreement with the porous distribution shown in Fig. 1, the sharpness of

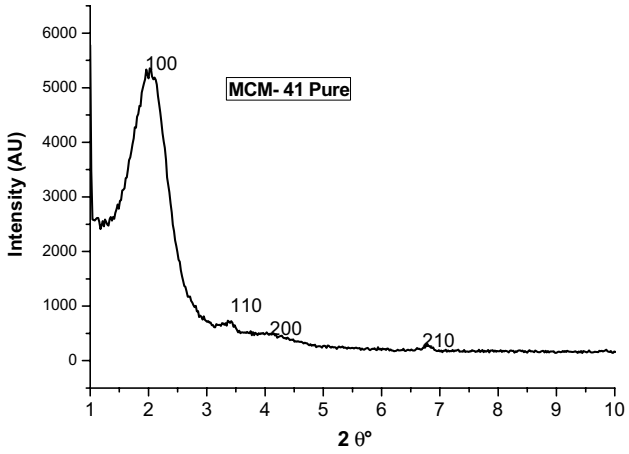

Fig. 3 XRD pattern of pure-silica MCM-41

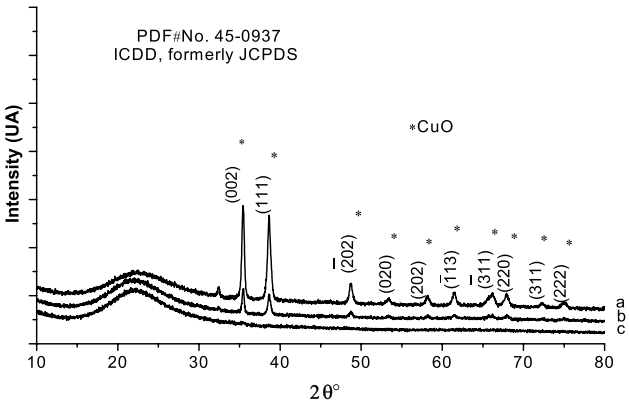

Fig. 4 XRD patterns of calcined: (*a*) 10-Cu/MCM-41, (*b*) 50-Cu/MCM-41, and (*c*) pure-silica MCM-41

the inflection step observed on the 10-Cu/MCM-41 catalyst reflects a uniform distribution of pore size, and the P/P_0 position is clearly related to the diameter in the mesopore range. For the 50-Cu/MCM-41 catalyst, this inflection step is lower which revealed a less uniform distribution of the pore size. The second step in the isotherms at relative pressure $P/P_0 > 0.8$, observed on *n*-Cu/MCM-4 catalysts, is attributed to the condensation of nitrogen in the depressions of rough surface or between small particles [31].

XRD is one of the most-used techniques to identify the structure of the MCM-41. This study made it possible to identify the crystalline phases present in the prepared catalysts. The powder X-ray diffraction patterns of MCM-41 and Cu impregnated MCM-41 samples are depicted in Figs. 3 and 4 in the range of 2θ = 1°–10° and 5°–80°, respectively. The general profile of the spectra obtained on all catalysts is typical of the pure phase MCM-41. Small-angle XRD patterns of all calcined catalysts show a broad sharp (100)

reflection peak in the 2θ range 1.5–2.5° (Fig. 3). Additional three broad peaks of low intensity at 2θ range 3.6°–6.8° is observed for (110), (200), and (210) planes, indicating a highly ordered hexagonal pore structure. The impregnation of copper on MCM-41 support did not affect the intensity of the (100), (110), (200), and (210) planes, implying that the totality of the metal ions have not been inserted into the silica framework. Based on Bragg's equation, the determination of d_{100} value [$\lambda = 2d_{100}\sin\theta$, with $\lambda = 1.5406$ A° from Cu(K_α)] was used for the calculation of the hexagonal unit cell parameter a_0 ($a_0 = 2d_{100}/\sqrt{3}$).

Knowing the values of a_0 and the pore diameter D_p($a_0 = D_p + t$), the pore wall thickness (t) can be deducted. The values of d-spacing, unit cell parameters, and pore wall thickness are given in Table 1. Similar values for d-spacing, wall thickness, and unit cell parameter were observed upon increasing the copper loading which suggests the absence of any incorporation of the metal cation into the silica framework location. This is also is in agreement with the presence of crystalline phases of metal oxides in the XRD diffraction patterns at high angles [32].

Figure 4 shows that the samples analyzed by XRD exhibit large silica peak around 23°, which suggests a low overall degree of crystallization of siliceous walls [33]. The appearance of several peaks of low intensities in the range 10°–80° can be attributed to the synthesis of crystalline copper oxides (CuO, JCPDS-ICDD card: 05-0661) located on the surface of the support and not in the pores of the catalysts [34]. The intensity of these peaks is increased by increasing the content of metal; this shows that the higher copper content involves an increase in the crystallinity phase and led to an increase in the crystallites size.

The FTIR spectra of as-synthesized MCM-41 and *n*-Cu/MCM-41 samples are shown in Fig. 5. The examination of the frequency range 450–4000 cm^{-1} in the spectra indicates the presence of vibrations bands that are similar and characteristic of the network silicate MCM-41. A broad band around at 3400 cm^{-1} is observed corresponding to the O–H stretching vibration of the adsorbed water molecules, whereas the bending vibration mode appears at 1630 cm^{-1}. The broad adsorption band observed around 1100 cm^{-1} is for the asymmetric stretching vibration of Si–O–Si bridge. The bands in the ranges 750–950 and 450–500 cm^{-1} are attributed to the symmetric stretching vibration of Si–O–Si bridge and Si–O bending vibration, respectively [35]. Furthermore, the impregnation of copper on MCM-41 material shows a modification in the intensity of the vibration bands at 450–1200 cm^{-1}. The decrease in the bands' intensity may be due to the presence of Si–O–Cu vibrations on the MCM-41 surface. The absence of absorption bands at 2800–3000 cm^{-1} corresponding to the absorptions of stretching and bending vibration modes of C–H bonds in the case of MCM-41 denotes the full elimination of the surfactant template CTAB after washing and calcination steps.

The morphology of 10-Cu/MCM-41 sample illustrated by the SEM image in Fig. 6 shows that the solids have a slightly homogeneous and crystalline pattern. The image shows also the presence of zones where the particles are assembled in paved clusters which shows that metal is not very well dispersed. Moreover, the presence of particles of copper and nickel more or less spherical assemblies in small aggregates can be well observed in the whole image.

3.2 Catalytic Results

It has been shown above that the various physicochemical techniques indicated that the copper species are not in framework positions in the prepared Cu/MCM-41 samples with a Si/Cu molar ratio of 10 and 50, and thereby, these species can be potentially active in the catalytic hydrogenation reactions. Here, we have carried out the reduction of benzaldehyde under hydrogen flow on Cu/MCM-41 samples at 160,

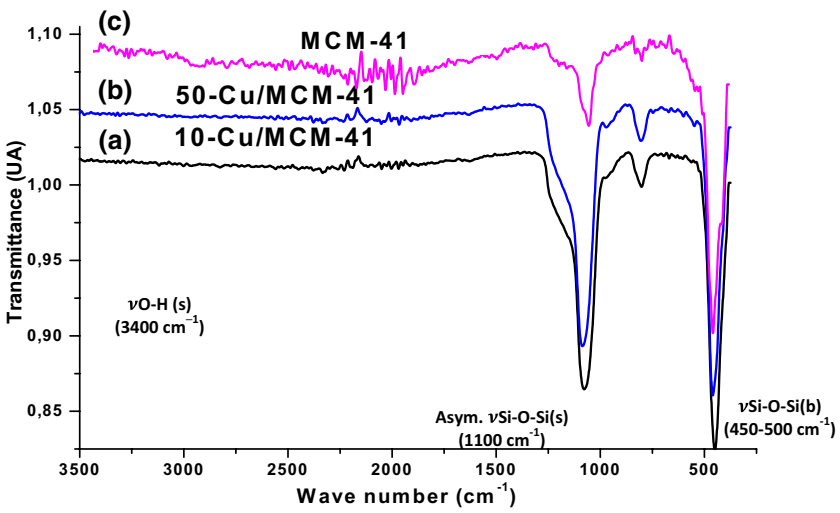

Fig. 5 FTIR spectra of: (*a*) 10-Cu/MCM-41, (*b*) 50-Cu/MCM-41, (*c*) pure-silica MCM-41

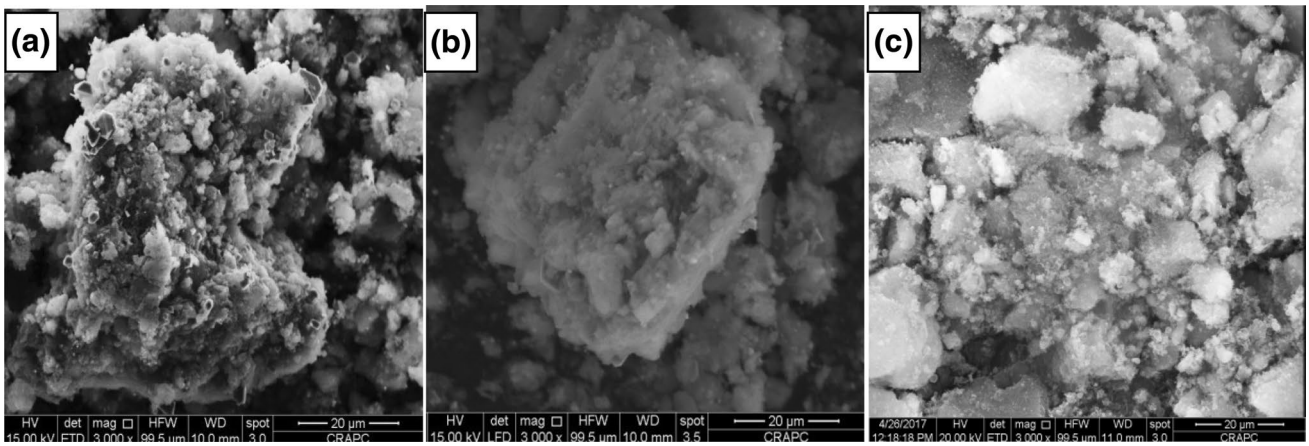

Fig. 6 SEM image of calcined: **a** 10-Cu/MCM-41, **b** 50-Cu/MCM-41, and **c** MCM-41 pure-silica

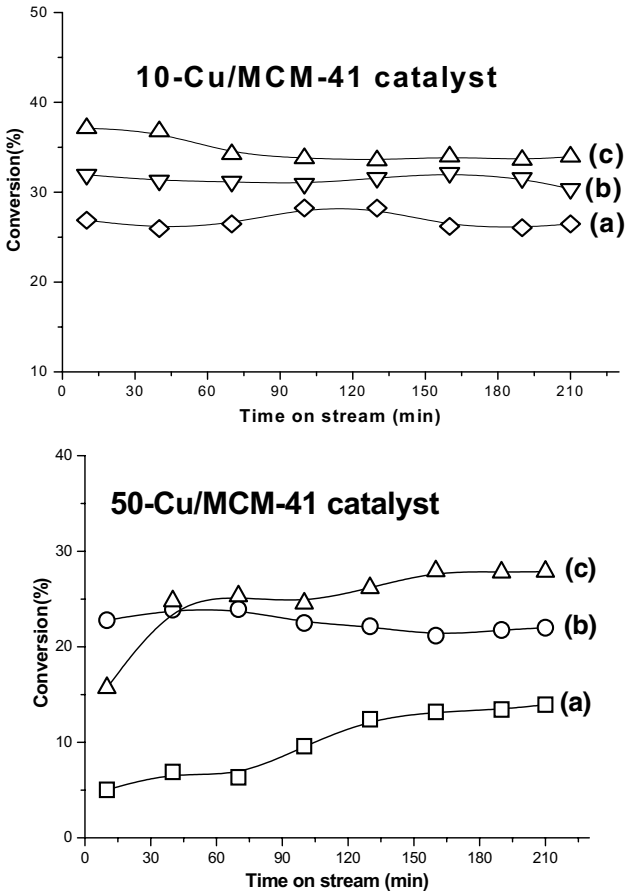

Fig. 7 Evolution of benzaldehyde conversion with time on stream over *n*-Cu/MCM-41 (n = Si/Cu = 10 and 50), pre-reduced temperature = 350 °C. Reaction temperature: (*a*) 160 °C, (*b*) 200 °C, (*c*) 250°C

Table 2 Catalytic results for benzaldehyde hydrogenation over *n*-Cu/MCM-41 catalysts

Catalyst	Temperature of reaction (°C)	Conversion[a] (%)	Selectivity[b] (%)		
			Benzyl alcohol	Toluene	Benzene
10-Cu/MCM-41	160	27	10	0	90
	200	32	19	0	81
	250	34	17	0	83
50-Cu/MCM-41	160	19	54	0	46
	200	22	72	9	19
	250	28	89	2	10

Reaction conditions: catalyst (25 mg), benzaldehyde (4.8 torr), H_2 (250 torr)

[a]Determined by GC based on benzaldehyde at steady state

[b]Determined by GC at steady state

200, 250 °C, and the obtained results are plotted in Fig. 7 and summarized in Table 2.

Before reaction, the catalyst was in situ pre-reduced under hydrogen flow at 350 °C for 2 h. The reaction temperature was maintained constant throughout the handling until the stationary mode was reached. During this stage of the reaction, the catalysts became stable thanks to the balance between the adsorption/desorption speed of the reactant and products of the reaction.

The used MCM-41 as a support was totally inactive, whereas the copper-based supported catalysts were active and selective in the gas phase reduction of benzaldehyde yielding the hydrogenation products benzyl alcohol, toluene, and benzene (Scheme 1).

Figure 7 shows that the catalysts 10-Cu/MCM-41 and 50-Cu/MCM-41 were relatively stable and totally active in benzaldehyde hydrogenation at the whole reaction temperature range and the steady state was established after

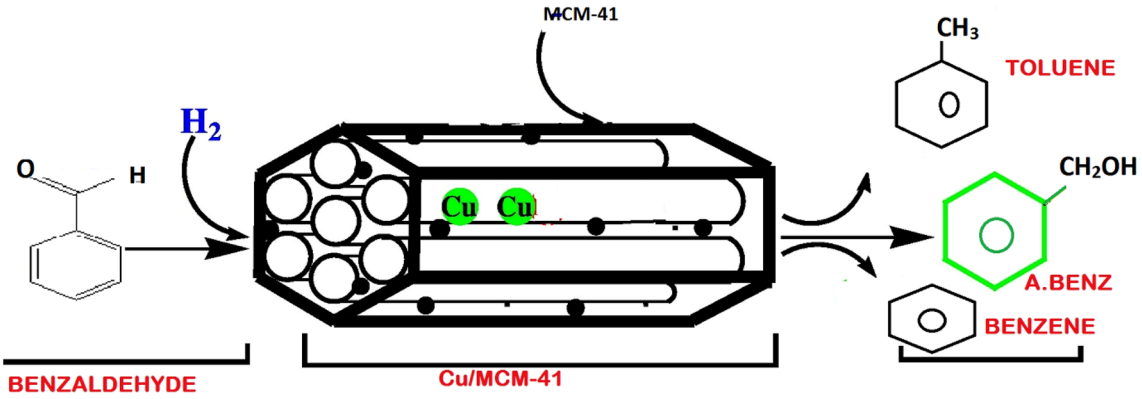

Scheme 1 Schematic representation of the reaction "reduction of benzaldehyde"

1 and 2 h reaction time on stream over the two catalysts, respectively. Furthermore, and regardless of the employed reaction temperature, the figure shows that 50-Cu/MCM-41 was the least active that exhibits an activation phenomenon with time on stream, whereas 10-Cu/MCM-41 was the most stable and active catalyst.

The steady-state activity and selectivity of the examined catalysts measured after 2 h of reaction time are listed in Table 2. The results show that the level and order of benzaldehyde conversion depended on both reaction temperature and copper weight on the MCM-41 support. The increase in the reaction temperature led to an increase in benzaldehyde conversion on both catalysts. At 200 °C, the conversion is 28% for a Si/Cu ratio of 50 and 34% for a Si/Cu = 10.

On the other hand, the conversion of benzaldehyde over *n*-Cu/MCM-41 catalysts at different Si/Cu ratios (n = Si/Cu = 50 and 10) and under the model reaction conditions was in the following order: 10-Cu/MCM-41 > 50-Cu/MCM-41. The high conversion of benzaldehyde over 10-Cu/MCM-41 compared to the 50-Cu/MCM-41 catalyst is probably attributed to the fact that the 10-Cu/MCM-41 catalyst exhibits higher copper crystallite sizes (Table 2).

The low activity of 50-Cu/MCM-41 catalyst which has the highest surface area and largest pore volume is mainly due to the presence of less number of active sites on the porous surface. The accessibility of the active sites by reactive molecules is directly related to the reducibility and the size of the copper particles located on the surface of the MCM-41 structure. For the most active catalyst 10-Cu/MCM-41, the possible presence of weak metal–support interaction could be the origin of the thick copper particles formation, which leads to a little dispersion of copper on the MCM-41 support. A similar observation has been reported in the case of the copper-supported catalysts [35], where we suggested that besides the reducibility properties, the acid–base properties of the catalysts would also be involved. FTIR study investigations have shown that the benzaldehyde adsorption on silica strengthens the hypothesis of the contribution of the acid–base properties and occurs through a hydrogen bond of the oxygen atom of the C=O group to the surface silanol groups [36, 37].

The reaction products (benzyl alcohol, toluene, and benzene) formed from benzaldehyde reduction are resulted from two types of reaction: (i) C=O double bond reduction to benzyl alcohol and toluene and (ii) C–C exocyclic bond hydrogenolysis to benzene. The study of the selectivity evolution of the reaction products according to the working time at the selected reaction temperature 250 °C is shown in Fig. 8.

The results showed that during the steady-state set-up at 250 °C, the reaction products are formed by different ways. With a high copper content (10-Cu/MCM-41), benzyl alcohol appeared as a primary product at the beginning of the reaction and its selectivity decreases with time, whereas benzene was formed independently and its selectivity tends to increase until the steady state was achieved. At low copper content, the behavior was totally different and benzyl alcohol was formed on the same site as benzene. At initial stages of the reaction, benzyl alcohol was not formed but began to appear with time as the selectivity of the benzene decreased. The steady-state selectivity of reaction products obtained from benzaldehyde hydrogenation for both catalysts is summarized in Table 2. The results show that the reduction of C=O function is observed in the range of reaction temperature (160–250 °C) and conducted to benzyl alcohol formation with high selectivity, whereas toluene appears with low selectivity only on 50-Cu/MCM-41 catalyst. The analysis of the results revealed that the high benzyl alcohol selectivities appeared on the least active catalyst due to the presence of low copper content. A strong metal–support interaction and high dispersion of copper on high specific surface area MCM-41 support would have played an important role. The formation of small copper particles may contribute to the high benzyl alcohol selectivity.

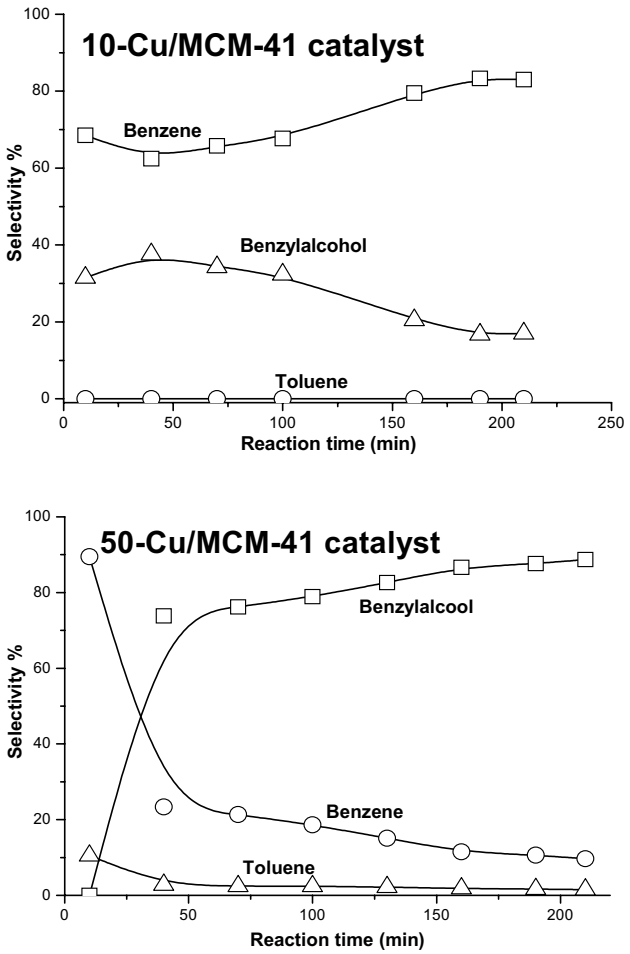

Fig. 8 Evolution of reaction products selectivity with time on stream at reaction temperature of 250 °C for *n*-Cu/MCM-41 (n = Si/Cu = 10 and 50)

Previous studies on the reducibility of copper particles by H_2-TPR method have shown that the appearance of several reduction steps is related to the presence of copper particles of different sizes in more or less strong interaction with support [38, 39]. It is well known that CuO phase can be reduced in the temperature range 230–500 °C [40], which may be related to the copper content, method of preparation, and the nature of the support. The highly dispersed copper species include isolated Cu^{2+} ions that strongly interact with the support, the isolated Cu^{2+} that weakly interact with the support (the cupric ions have close contact with each other), and small two-dimensional clusters or three-dimensional ones era reduced at low temperature region, whereas the reduction of larger and bulk CuO is observed at higher temperature region.

According to the literature, the benzyl alcohol formation from benzaldehyde reduction needs centers for both the activation and reduction of the carbonyl function. These specific sites would be involved, probably at the metal–support interfacial region [41, 42]. It was suggested that active sites were composed with a special ensemble of at least one metal cation adjacent to a defect site on the support [43], which would allow a chemical interaction between the oxygen atom in the carbonyl bond and the support thereby polarizing and activating the C=O bond towards hydrogen [44].

Toluene is considered as a product of consecutive reaction from benzyl alcohol hydrogenolysis [45] and it appeared as a secondary product at initial stages of the reaction (Fig. 8). The formation of toluene with a very low selectivity may be related to the presence of low copper content on MCM-41 support, which facilitated the desorption of benzyl alcohol with a very high amount rather than formation of toluene.

Benzene was formed in all reaction temperatures using both catalysts. The absence of the aromatic ring hydrogenation products may indicate the lack of any catalytically active species for benzene hydrogenation under the employed reaction conditions, even at low reaction temperature. On the other hand, the study of the selectivity of the reaction as a function of time on stream showed that benzene was also detected as a primary product (Fig. 8) and its formation was following an independent route from those obtained from the reduction of C=O functionality. The high selectivities obtained using the 10-Cu/MCM-41 catalyst at all tested reaction temperatures are due to the formation of large copper particles into the additional framework of MCM-41.

4 Conclusion

Copper-based catalysts supported on MCM-41 silica were prepared by an impregnation method. The XRD patterns and nitrogen physisorption analyses confirmed the existence of ordered mesoporous silica and the degree of copper species dispersion on the ordered mesoporous hexagonal MCM-41 mesoporous molecular sieves was obtained with the low Cu content (Si/Cu = 50), while a remarkable low dispersion was obtained on the 10-Cu/MCM-41 catalyst attributed to the formation of large crystallite size. Both catalysts, 10-Cu/MCM-41 and 50-Cu/MCM-41, showed different catalytic activity and stability in the gas phase hydrogenation of benzaldehyde. The catalytic activity of 50-Cu/MCM-41 catalyst was lower than that of 10-Cu/MCM-41 and no significant deactivation was found during the stability test. This high stability was attributed to the thermal stability of the MCM-41 structure. The formation of well-dispersed copper particles on 50-Cu/MCM-41 favored the benzyl alcohol as principal reaction product. Oppositely, the high copper content present on 10-Cu/MCM-41 catalyst oriented the reaction towards the formation of benzene as the major hydrogenolysis product.

References

1. Chen HL, Zhang K, Wang YM (2012) Steam-assisted crystallization of TPA+ -exchanged MCM-41 type mesoporous materials with thick pore walls. Mater Res Bull 47:1774–1782. https://doi.org/10.1016/j.materresbull.2012.03.029
2. Ni M, Leung DYC, Leung MKH, Sumathy K (2006) An overview of hydrogen production from biomass. Fuel Process Technol 87:461–472. https://doi.org/10.1016/j.fuproc.2005.11.003
3. Herrmann J (1999) Heterogeneous photocatalysis: fundamentals and applications to the removal of various types of aqueous pollutants. Catal Today 53:115–129. https://doi.org/10.1016/S0920-5861(99)00107-8
4. Phalguni C, Claudio NV, Eckhard B, Eberhard B, Thomas W, Karl W (2001) Electronic structure of bis(o-iminobenzosemiquinonato)metal complexes (Cu, Ni,Pd) the art of establishing physical oxidation states in transition-metal complexes containing radical ligands. J Am Chem Soc 123:2213–2223. https://doi.org/10.1021/ja003831d
5. Christian Enger B, Lødeng R, Holmen A (2008) A review of catalytic partial oxidation of methane to synthesis gas with emphasis on reaction mechanisms over transition metal catalysts. Appl Catal A 346:1–27. https://doi.org/10.1016/j.apcata.2008.05.018
6. Patel S, Patel M (1991) DTA of some reduceable metal ion exchanged montmorillonites. J Therm Anal 37:667–670. https://doi.org/10.1007/BF01913118
7. Kresge CT, Leonowicz ME, Roth WJ, Vartuli JC, Beck JS (1992) Ordered mesoporous molecular sieves synthesized by a liquid-crystal template mechanism. Nature 359:710–712. https://doi.org/10.1038/359710a0
8. Beck JS, Vartuli JC, Roth WJ, Leonowickz ME, Kresge CT, Schmitt KD, Chu TW, Olson DH, Sheppard EW, McCullen SB, Higgins JB, Lshlenker (1992) A new family of mesoporous molecular sieves prepared with liquid crystal templates. J Am Chem Soc 114:10834–10843. https://doi.org/10.1021/ja00053a020
9. Vartuli JC, Schmitt KD, Kresge CT, Roth WJ, Leonowicz ME, McCullen SB, Hellring SD, Beck JS, Schlenker JL, Olson DH, Sheppardt EW (1994) Effect of surfactant/silica molar ratios on the formation of mesoporous molecular sieves: inorganic mimicry of surfactant liquid-crystal phases and mechanistic implications. Chem Mater 6:2317–2326. https://doi.org/10.1021/cm00048a018
10. Kapoor MP, Inagaki S (2006) Highly ordered mesoporous organosilica hybrid materials. Bull Chem Soc Jpn 79:1463–1475. https://doi.org/10.1246/bcsj.79.1463
11. Parida KM, Dash SS (2009) Manganese containing MCM-41: synthesis, characterization and catalytic activity in the oxidation of ethylbenzene. J Mol Catal A 306:54–61. https://doi.org/10.1016/j.molcata.2009.02.022
12. Sakthivel A, Selvam P (2002) Mesoporous (Cr)MCM-41: a mild and efficient heterogeneous catalyst for selective oxidation of cyclohexane. J Catal 211:134–143. https://doi.org/10.1006/jcat.2002.3711
13. Carvalho WA, Wallau M, Schuchardt U (1999) Iron and copper immobilised on mesoporous MCM-41 molecular sieves as catalysts for the oxidation of cyclohexane. J Mol Catal A 144:91–99. https://doi.org/10.1016/S1381-1169(99)00031-X
14. Abd Hamid SB, Ambursa MM, Sudarsanam P, Voon LH, Bhargava SK (2017) Effect of Ti loading on structure-activity properties of Cu-Ni/Ti-MCM-41 catalysts in hydrodeoxygenation of guaiacol. Catal Commun 94:18–22. https://doi.org/10.1016/j.catcom.2017.02.006
15. Saadi A, Merabti R, Rassoul Z, Bettahar MM (2006) Benzaldehyde hydrogenation over supported nickel catalysts. J Mol Catal A 253:79–85. https://doi.org/10.1016/j.molcata.2006.03.003
16. Beller M, Bolm C (2004) Frontmatter. In: Transition metals for organic synthesis, Second Rev. Wiley, Weinheim, pp I–XIX
17. Nishimura S (2001) Handbook of heterogeneous catalytic hydrogenation for organic synthesis. Wiley, New York. https://doi.org/10.1021/op0100798
18. Pugh S, Mckenna R, Halloum I, Nielson DR (2015) Engineering *Escherichia coli* for renewable benzyl alcohol production. Metab Eng Commun 2:39–45. https://doi.org/10.1016/j.meteno.2015.06.002
19. Scognamoglio J, Jones L, Vitale D, Letizia CS, Api AM (2012) Enhanced production of benzyl alcohol in the gas phase continuous hydrogenation of benzaldehyde over Au/Al_2O_3. Food Chem Toxicol 50:S140–S160. https://doi.org/10.1016/j.catcom.2013.12.024
20. Li M, Wang X, Perret N, Keane MA (2014) Fragrance material review on benzyl alcohol. Catal Commun 46:187. https://doi.org/10.1016/j.fct.2011.10.013
21. Bhanushali TJ, Kainthla I, Keri SK, Nagaraja BM (2016) Catalytic hydrogenation of benzaldehyde for selective synthesis of benzyl alcohol: a review. ChemistrySelect. https://doi.org/10.1002/slct.201600712
22. Hii PJ, Krische KK, Mr JW (2013) Sustainable catalysis. Wiley, Hoboken
23. Rylander P, Ullmann's PN (2005) Encyclopedia of industrial chemistry. Wiley, Weinheim
24. Claus P (1998) Selective hydrogenation of ά,β-unsaturated aldehydes and other C=O and C=C bonds containing compounds. Top Catal 5:51–62. https://doi.org/10.1023/A:1019177330810
25. Parida KM, Rath D (2007) Structural properties and catalytic oxidation of benzene to phenol over CuO-impregnated mesoporous silica. Appl Catal A 321:101–108. https://doi.org/10.1016/j.apcata.2007.01.054
26. Selvam P, Bhatia SK, Sonwane CG (2001) Recent advances in processing and characterization of periodic mesoporous MCM-41 silicate molecular sieves. Ind Eng Chem Res 40:3237–3261. https://doi.org/10.1021/ie0010666
27. Wu Q, Hu X, Yue PL, Zhao XS, Lu GQ (2001) Copper/MCM-41 as catalyst for the wet oxidation of phenol. Appl Catal B 32:151–156. https://doi.org/10.1016/S0926-3373(01)00131-X
28. Guinier A (1994) X-ray diffraction in crystals, imperfect crystals, and amorphous bodies. Dover, New York
29. Everett DH (1972) Manual of symbols and terminology for physicochemical quantities and units, appendix II: definitions, terminology and symbols in colloid and surface chemistry. Pure Appl Chem. https://doi.org/10.1351/pac197231040577
30. Vetrivel S, Pandurangan A (2005) Co and Mn impregnated MCM-41: their applications to vapour phase oxidation of isopropylbenzene. J Mol Catal A 227:269–278. https://doi.org/10.1016/j.molcata.2004.10.036
31. Dong X, Shen W, Zhu Y, Xiong L, Gu J, Shi J (2005) Investigation on Mn-loaded mesoporous silica MCM-41 prepared via reducing KMnO4 with in situ surfactant. Microporous Mesoporous Mater 81:235–240. https://doi.org/10.1016/j.micromeso.2005.02.006
32. Liu D, Quek XY, Cheo WNE, Lau R, Borgna A, Yang Y (2009) MCM-41 supported nickel-based bimetallic catalysts with superior stability during carbon dioxide reforming of methane: effect of strong metal–support interaction. J Catal 266:380–390. https://doi.org/10.1016/j.jcat.2009.07.004
33. Derylo-Marczewska A, Gac W, Popivnyak N, Zukocinski G, Pasieczna S (2006) The influence of preparation method on the structure and redox properties of mesoporous Mn-MCM-41 materials. Catal Today 114:293–306. https://doi.org/10.1016/j.cattod.2006.02.066

34. (1991) Joint committee on powder diffraction standards, diffraction data file, no. 45–0937. In: International centre for diffraction data. (ICDD, formerly JCPDS), Newtown Square, PA
35. Saadi A, Rassoul Z, Bettahar M (2000) Gas phase hydrogenation of benzaldehyde over supported copper catalysts. J Mol Catal A 164:205–216. https://doi.org/10.1016/S1381-1169(00)00199-0
36. Koutstaal C (1993) Surface chemistry of benzoyl compounds on oxides, an FT-IR study. J Catal 143:573–582. https://doi.org/10.1006/jcat.1993.1300
37. Merabti R, Bachari K, Halliche D, Rassoul Z, Saadi A (2010) Synthesis and characterization of activated carbon-supported copper or nickel and their catalytic behavior towards benzaldehyde hydrogenation. React Kinet Mech Catal 101:195–208. https://doi.org/10.1007/s11144-010-0215-x
38. Dow W-P, Wang Y-P, Huang T-J (1996) Yttria-stabilized zirconia supported copper oxide catalyst. J Catal 160:155–170. https://doi.org/10.1006/jcat.1996.0135
39. Dow W-P, Wang Y-P, Huang T-J (2000) TPR and XRD studies of yttria-doped ceria/γ-alumina-supported copper oxide catalyst. Appl Catal A 190:25–34. https://doi.org/10.1016/S0926-860X(99)00286-0
40. Wang Z, Liu Q, Yu J, Wu T, Wang G (2003) Surface structure and catalytic behavior of silica-supported copper catalysts prepared by impregnation and sol–gel methods. Appl Catal A 239:87–94. https://doi.org/10.1016/S0926-860X(02)00421-0
41. Hubaut R (1992) Study of the competitive reactions between an α-β-unsaturated aldehyde and allylic alcohol on a copper chromite catalyst. React Kinet Catal Lett 46:25–32. https://doi.org/10.1007/BF02096673
42. Daage M, Bonnelle JP (1985) Selective hydrogenation of dienes on copper-chromite catalysts III reaction mechanism and nature of the occluded hydrogen species. Appl Catal 16:355–374. https://doi.org/10.1016/S0166-9834(00)84399-7
43. Vannice MA, Sudhakar C (1984) A model for the metal-support effect enhancing carbon monoxide hydrogenation rates over platinum-titania catalysts. J Phys Chem 88:2429–2432. https://doi.org/10.1021/j150656a002
44. Vannice MA (1992) Hydrogenation of co and carbonyl functional groups. Catal Today 12:255–267. https://doi.org/10.1016/0920-5861(92)85044-M
45. Haffad D, Kameswari U, Bettahar MM, Chambellan A, Lavalley JC (1997) Reduction of benzaldehyde on metal oxides. J Catal 172:85–92. https://doi.org/10.1006/jcat.1997.1854